Theoretical Dimensioning and Sizing Limits of Hybrid Energy Storage Systems

Sebastian Günther[a], Astrid Bensmann[a,*], Richard Hanke-Rauschenbach[a]

[a]*Department of Electrical Energy Storage Systems, Leibniz Universität Hannover, Appelstr. 9A, 30167 Hannover, Germany*

Abstract

Aim of a storage hybridisation is a beneficial usage or combination of different storage technologies with various characteristics to downsize the overall system, decrease the costs or to increase the lifetime, system efficiency or performance. In this paper, the point of interest is a different ratio of power to energy (specific power) of two storages to create a hybrid energy storage system (HESS) with a resulting specific power that better matches the requirements of the application. The approach enables a downsizing of the overall system compared to a single storage system and consequently decreases costs. The paper presents a theoretical and analytical benchmark calculation, which determines the maximum achievable hybridisation, i.e. possible spread in specific power, while retaining the original total energy and power capacities of an equivalent single storage system. The theory is independent from technology, topology, control strategy, and application and provides a unified view on hybrid energy storage systems. It serves as a pre-dimensioning tool and first step within a larger design process. Furthermore, it presents a general approach to choose storage combinations and to characterize the potential of an application for hybridisation. In this context, a Hybridisation Diagram is proposed and integral Hybridisation Parameters are introduced.

Keywords: hybrid energy storage systems, dimensioning, sizing, pre-dimensioning, hybridisation potential

1. Introduction

To this date, electric energy storage systems are generally expensive. This creates the need for an effective utilisation of energy storages. Since all available storage technologies have differing characteristics regarding their power and energy density, specific power, response time, efficiency, self-discharge rate, cycle stability, life expectancy or aging behaviour, they come with different advantages or disadvantages and are therefore more or less suited for certain applications [1, 2, 3].

Within the field of HESS, it is tried to combine different storage technologies to generate a system with an increased performance regarding the aforementioned parameters. A common approach is to complement a high energy storage with slow response rate (e.g. a battery) with a high power storage with fast response rate (e.g. a super capacitor) [2]. This way, the power density and response rate of the system is increased. Moreover, the number of cycles and the stress induced by high transients can be reduced, leading in turn to a smaller size and longer life time compared to the battery-alone system, which also reduces costs [1, 2].

To achieve this goal, a major research subject within the field of HESS is control, which addresses the distribution of power and energy between the storages. It includes filter-based, rule-based or model predictive control strategies as well as fuzzy controllers, neural networks or combinations of them [2]. Topological studies, including passive, semi-active, and active power electronics, are also common [2] and battery-supercapacitor combinations in automotive, regenerative power or pulsed load applications are widely investigated [2, 4].

Most studies do not focus on dimensioning explicitly. It is rather only a consequence and not considered solely. The simultaneous treatment of control strategy, topology and dimensioning seems to be reasonable since they are all interdependent, yet, it blurs the view for a comprehensive system design. Either, dimensioning is made with an inherent control strategy [5, 6, 7, 8, 9], or generic global optimizations are performed [10, 11, 12, 13, 14, 15] with the drawback of hiding the influence of the design variables. Moreover, simulations are carried out with detailed storage models, which makes the results less general and applicable to similar problems.

The aim of this paper is to provide a general top level view on HESS, allowing an investigation of the dimensioning problem independent of technology, control strategy, and application. From energetic considerations, every application has a inherent power and energy demand, and consequently a specific power. Storages seldomly fit this specific power, it is either too high or too low, which leads to an overdimensioning in power or energy capacity. This paper presents a theory that allows the combination of two storage technologies with varying specific powers to generate an HESS with a resulting specific power that lies in between and matches the requirements of the application, and in return reduces the size of the overall storage system. Afterwards, a beneficial mapping to existing storage technologies is easily possible. It is an analytical approach that solely considers the specific power by neglecting storage specific nonidealities such as system response times or cycle stability. By itself, it does not inherently improve any of these criteria. It is intended as a pre-dimensioning tool within a larger design process and

*Corresponding author. Tel.: +49 511 762 14410, astrid.bensmann@ifes.uni-hannover.de

subsequent analysis have to address the aforementioned issues.

The paper is structured as follows: First, a thorough description of the idea and its resulting insights are presented in Section 2. The underlying model is deferred to Section 3. Note, that this section is not obligatory for the understanding and usage of the theory and its results, and can be omitted from the users point of view. An expansion of the theory, which provides a mapping of the results to specific technologies and allows an economic investigation, is shown in Section 4. In Section 5, the theory is applied to two examples before the paper is concluded and summarized in Section 6.

2. General Theory Description

This section presents the idea, insights, limitations and value of the theory without a formal mathematical introduction. In this way, the purpose becomes clearer and the model and derivations presented in the following section can be understood more easily.

2.1. Idea and Aim

For a given periodic power profile of the storage system, hereinafter referred to as signal, the required power capacity P_s and energy capacity E_s of a single storage can be determined easily. By neglecting losses and other nonidealities, the required power capacity P_s is the maximum of that signal and the required energy capacity E_s is the maximum of the integral of that signal. The signal must be handled by the storage system and the control strategy or energy management system is not allowed to dismiss provided or required power.

It is assumed that no storage exists that has the specific power required by these considerations. Therefore, the single storage, which acts as a reference shall now be split into two hybrid storages, namely a base and a peak storage. The power capacity of the base storage P_b is a fraction $\chi \in [0, 1]$ of the single storage power capacity P_s and the peak storage power capacity P_p is determined by the residual fraction $(1-\chi)$ of the single storage power capacity P_s. Consequently, the powers P_b and P_p of the base and peak storages add up to the power of the single storage P_s. The dimensioning of the energy capacities of base and peak storages shall fulfil the same requirement: Base storage energy capacity E_b and peak storage energy capacity E_p shall add up to the single storage energy capacity E_s. Further, for a given fraction or power cut χ, the peak storage energy E_p shall become minimal in a way that control strategies still exist that can distribute the power between the two storages without exceeding the energy and power capacities of the storages at some point in time.

A control strategy, which preserves the energy and power capacities of the single storage system while minimizing the energy capacity of the peak storage, can be formulated verbally as follows: The peak storage shall be only charged if necessary, i.e. when the input power exceeds the power capacity of the base storage, and shall be discharged whenever possible. Some exceptions exist to ensure a failsafe operation. They are presented within the mathematical formulation in Section 3.

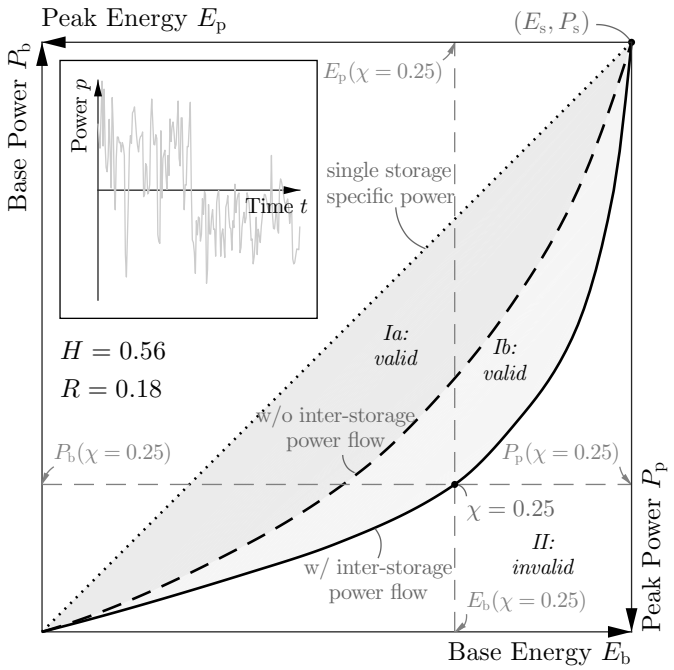

Figure 1: Hybridisation Curve in $P(E)$-diagram; Note the two coordinate systems, where the first regular one represents base storage, and the second one is rotated by 180° and translated to the point of the single storage for representation of peak storage. For a power cut χ, the base and peak storage sizes can be read in the according coordinate systems.

2.2. Insights and Consequences

A single storage that fulfills the requirements of a given signal can always be separated into a base and a peak storage, whose power capacities $(P_\mathrm{b}, P_\mathrm{p})$ and energy capacities $(E_\mathrm{b}, E_\mathrm{p})$ add up to the power capacity P_s and energy capacity E_s of the single storage. Moreover, the introduced control strategy minimizes the energy capacity E_p of the peak storage. This way, the specific powers of the two storages

$$\omega_i(\chi) = \frac{P_i(\chi)}{E_i(\chi)} \qquad i \in \{\mathrm{b}, \mathrm{p}\} \tag{1}$$

are spread as much as possible, providing more potential of using different storages with regard to their specific power. The introduced specific power ω is similar to the C-Rate commonly used for the characterisation of batteries. However, the C-Rate relates current to capacity. In this paper, it is generalized by relating power to energy. The specific power of the base storage ω_b is always lower than that of the original single storage ω_s and the specific power of the peak storage ω_p is always higher.

Each power cut χ generates a tuple of base and peak storages, which can be represented in a $P(E)$–diagram called Hybridisation Diagram, as shown in Fig. 1. The axes are limited to the dimension of the single storage, i.e. power and energy capacities P_s and E_s. The dotted diagonal line is the specific power line of the single storage, which fulfils the requirement of the signal.

The solid Hybridisation Curve in Fig. 1 represents the dimension of the base storage as a function of the power cut χ (χ is the parameter of that curve) that is optimal in the sense of

the minimization described above. Since base and peak storage dimensions add up to the single storage dimension, the dimension of the peak storage is the difference between base storage and single storage. Therefore, a second rotated and translated coordinate system can be introduced, as shown in Fig. 1 (upper right axes), to represent the dimension of the peak storage with the same solid line. To determine the dimension of the base storage, read the E and P values in the bottom left coordinate system, and to determine the dimension of the peak storage, read the values in the top right coordinate system. For example, for a power cut of $\chi = 0.25$, base and peak storages have the following dimensions:

$$\chi = 0.25 \quad \mapsto \quad \begin{pmatrix} P_\mathrm{b} = 0.25 P_\mathrm{s} & E_\mathrm{b} \approx 0.7 E_\mathrm{s} \\ P_\mathrm{p} = 0.75 P_\mathrm{s} & E_\mathrm{p} \approx 0.3 E_\mathrm{s} \end{pmatrix}$$

Following, for this power cut $\chi = 0.25$, the single storage is replaced by a base storage with a specific power of

$$\omega_\mathrm{b} = \frac{0.25}{0.7}\,\omega_\mathrm{s} = 0.36\,\omega_\mathrm{s}$$

and a peak storage with a specific power of

$$\omega_\mathrm{p} = \frac{0.75}{0.3}\,\omega_\mathrm{s} = 2.5\,\omega_\mathrm{s} \quad .$$

The dashed line has a similar meaning as the solid line, but results from a modified control strategy. In case of the solid line, a power flow between the storages is allowed, i.e. the peak storage can discharge its energy into the base storage or vice versa. In case of the dashed line, this kind of inter-storage power flow is forbidden, i.e. the storages can only charge or discharge within the limits of the signal.

The dotted specific power line of the single storage and the solid, respectively dashed Hybridisation Curve enclose an area *(Ia)* or *(Ib)*, respectively. Within the areas, all tuples of storages are valid with respect to the requirement that base and peak storage dimensions add up to the single storage dimension. The solid and dashed line by themselves mark the optimal points with respect to the minimization of the energy of the peak storage for a certain power cut χ. The storage tuples outside area *(I)*, namely area *(II)*, are invalid in the sense that they cannot fulfil the requirements of the signal, i.e. no control strategy exists that can distribute the signal to the base and peak storages in a way that their power and/or energy capacities are not exceeded at some point in time. An additional overdimensioning would be necessary. Here, overdimensioning means that the sum of the energies (E_b, E_p) and/ or powers (P_b, P_p) of the base and peak storages is larger than the values of the single storage E_s and P_s. This aspect is further advanced in Section 4.

Additional information are provided in the Hybridisation Diagram in Fig 1. First, a visual representation of the analyzed signal is given as an inset in a power over time diagram (upper left corner). Further, the characteristic numbers H and R with respect to the hybridisation are given. These are defined as follows:

$$H = 2 \int_0^1 \frac{E_\mathrm{b}(\chi)}{E_\mathrm{s}} \mathrm{d}\chi - 1 \tag{2}$$

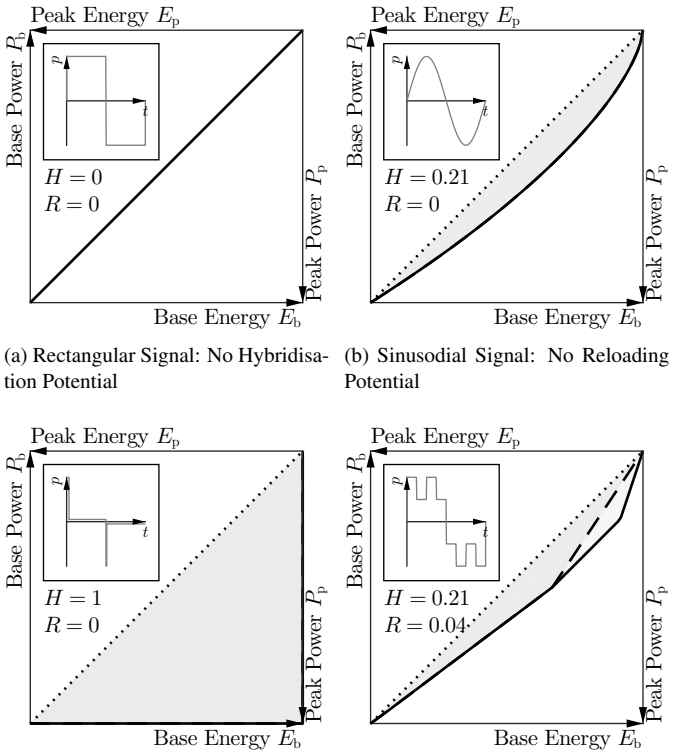

(a) Rectangular Signal: No Hybridisation Potential

(b) Sinusodial Signal: No Reloading Potential

(c) Dirac-alike Signal: Maximum Possible Hybridisation

(d) Stair Signal: Hybridisation curve as piecewise linear function

Figure 2: Various signals that show a degenerated Hybridisation Curve.

$$R = H - H^* \tag{3}$$

The Hybridisation Potential $H \in [0, 1]$ describes the normalized area *(Ia)* and *(Ib)* of valid storage tuples in Fig. 1. It is the fraction of valid tuples related to all tuples. The Reloading Potential $R \in [0, 1]$ describes the absolute gain of the Hybridisation Potential H through inter-storage power flow. In (3), H^* is the Hybridisation Potential where the inter-storage power flow is forbidden, or the normalized area *(Ia)*, respectively. For the arbitrary signal in Fig. 1, the Hybridisation Potential is $H = 0.56$, meaning that 56 % of the possible HESS-tuples can handle the signal without exceeding its energy and power capacities, while the remaining 44 % cannot handle it and would violate the constraints. Without an allowed inter-storage power flow between the two storages, 18 % less tuples would be valid, as the Reloading Potential is $R = 0.18$.

The shape of the Hybridisation Curve is signal dependend. Generally, signals with larger form and crest factors lead to a more distinct Hybridisation Curve and therefore higher Hybridisation Potential, although a bijective functional relationship proved to be wrong. For some signals, the Hybridisation Curve can degenerate, as shown in Fig. 2. For a rectangular signal (Fig. 2a), the Hybridisation Curve becomes a straight line equivalent to the specific power line of the single storage. Then, no hybridisation is possible. Other signals do not have a Reloading Potential, such as a simple Sine Signal (Fig. 2b). For a Dirac-impulse that is superposed by a rectangular function (Fig. 2c), the Hybridisation Potential tends towards 1 and for

piecewise-defined functions (Fig. 2d), the Hybridisation Curve becomes piecewise-defined, as well.

2.3. Limitations and Value

Although the concept presented and furtherly detailed within the next section is analytical and complete, it abstracts the problem to a solely energetic balance by neglecting several real-life aspects like losses, aging, power degradations, system response rates and other nonidealities. Moreover, an omniscient control strategy would be required in most cases, making it hard to apply without modification.

A unified dimensioning and design process, independent of the application or scale of the problem, is the benefit of these simplifications. It separates the dimensioning problem from the control strategy, providing a top level view and giving insight to the nature of the problem with the help of the proposed Hybridisation Diagram in Fig. 1 and its resulting parameters in (2) and (3). With this, it acts as a pre-dimensioning tool and it determines the potential of a signal for hybridisation. Sections 4 and 5 show how different technology combinations can be analyzed and compared. A first cost estimation is possible with the help of the theory, which can provide reasoning for more thorough investigations. It can help finding a good starting point of subsequent optimizations or can help determining a favourable control strategy. The theory is not intended to be a standalone design tool but a first step of a thorough system design. It does not contradict previous work within the field of HESS but shall support the hybrid energy storage design process within a larger framework.

3. Detailed Mathematical Framework

In this section, the mathematical and modelling background of the previous section is provided. After stating the requirements and assumptions of the calculation, the dimensioning algorithm is presented followed by the control strategy that guarantees a valid operation.

3.1. Problem Definition

A dimensioning and control strategy shall be found that satisfies

$$\begin{aligned} P_\mathrm{b}(\chi) + P_\mathrm{p}(\chi) &= P_\mathrm{s} \quad \wedge \\ E_\mathrm{b}(\chi) + E_\mathrm{p}(\chi) &= E_\mathrm{s} \quad \forall \chi \in [0,1] \quad . \end{aligned} \tag{4}$$

The capitalized variable P denotes power capacity, variable E the energy capacity of a storage. Subscripts b, p, and s denote base, peak, and single storage. Variable χ denotes the power cut as a fraction of base storage power related to single storage power:

$$\chi = \frac{P_\mathrm{b}}{P_\mathrm{s}} \tag{5}$$

Uncapitalized variables e and p denote the instantaneously stored energy and instantaneous power, respectively, and therefore depend on time t. It shall apply:

$$\begin{aligned} p(t) = p_\mathrm{s}(t) \quad \wedge \quad p_\mathrm{s}(t) = p_\mathrm{b}(t) + p_\mathrm{p}(t) \quad \forall t \\ e(t) = e_\mathrm{s}(t) \quad \wedge \quad e_\mathrm{s}(t) = e_\mathrm{b}(t) + e_\mathrm{p}(t) \quad \forall t \end{aligned} \tag{6}$$

Variable p without an index denotes the load or signal that the hybrid storage system is required to handle. Power p and energy e are related by

$$e(t) = \int_0^t p(\vartheta)\,\mathrm{d}\vartheta \quad . \tag{7}$$

Additionally, p_b, p_p, e_b and e_p must satisfy

$$\begin{aligned} -P_i \leq p_i(t) \leq P_i \quad \wedge \\ 0 \leq e_i(t) \leq E_i \quad \forall t, \quad i \in \{\mathrm{b}, \mathrm{p}\} \quad . \end{aligned} \tag{8}$$

This means that a control strategy must ensure that the instantaneous powers and energies stay within the power and energy capacities of the storages. With this equation, the assumption is made that the maximum charging power equals the maximum discharging power. This is not a necessary restriction but makes the results easier to interpret. It is aimed to maximize the spread in specific powers, i.e. the ratio $\omega_\mathrm{p}/\omega_\mathrm{b}$, for a fixed power cut χ. This yields storages that mostly differ regarding this parameter, which is interpreted as a higher potential for hybridisation. Since the power capacities P_b and P_p are already fixed for a given power cut χ, the result is obtained by maximizing the energy capacity of the base storage or minimizing the energy capacity of the peak storage:

$$\begin{aligned} \min \quad & E_\mathrm{p}(\chi) \quad \forall \chi \in [0,1] \\ \text{s. t. :} \quad & (4), (6), (8) \end{aligned} \tag{9}$$

It is sufficient to formulate this minimization for one storage, as minimizing one storage leads with (4) to maximizing the other one. It is also possible to minimize the base power capacity E_b leading to mirrored results, though this would undermine the meanings of “base” and “peak”.

3.2. Assumptions

To allow an analytic solution of the problem, a few assumptions were made or are already inherently made in the problem definition. First, the signal must be periodic:

$$p(t) = p(t+T) \quad \forall t \tag{10}$$

This is a relatively soft requirement but emphasizes that the dimensioning is only guaranteed to hold if the signal does not change. Moreover, the arithmetic mean must be zero:

$$\int_0^T p\,\mathrm{d}t = 0 \tag{11}$$

From (6) follows that there are neither conversion losses nor stand-by losses. Equation (11) is with regard to (10) a logical consequence since the State Of Charge $\mathrm{SOC}_i = e_i/E_i$, $i \in \{\mathrm{b}, \mathrm{p}\}$ of each storage must be periodic, as well. Otherwise, they would infinitely charge or discharge within time. Thus, the arithmetic mean of p_b and p_p is zero, too. Further, it shall hold that

$$e(t=0) = 0 \quad \wedge \quad e \geq 0 \quad \forall t \quad . \tag{12}$$

This is no restriction since a periodic signal must have a repetitive global minimum if it does not diverge, which is true for

physical realizable functions. Then, the signal can always be shifted within t-coordinate in a way that the minimum of energy is at the beginning of the period. An important consequence of (12) with (4) is that both storages must be completely empty at least at the beginning and the end of a period, and there must be at least one point within a period where both storages are completely charged:

$$\begin{aligned} e_i(t=0) = e_i(t=T) = 0 \quad \wedge \\ e_i(t=t^*)/E_i = 1 \quad \forall i, \quad i \in \{\mathrm{b}, \mathrm{p}, \mathrm{s}\} \end{aligned} \tag{13}$$

Otherwise, the system would be overdimensioned in comparison to the single storage, violating the requirement in (4).

Summarizing, the main limitations resulting from the problem definition and assumptions is that the storages do not have any losses and the signal has to be handled by the storages and is not allowed to be curtailed or modified.

3.3. Dimensioning

Determining the required power capacities for a certain power cut χ is trivial since (4) and (5) immediately lead to

$$\begin{aligned} P_\mathrm{b}(\chi) &= \chi P_\mathrm{s} \\ P_\mathrm{p}(\chi) &= (1-\chi) P_\mathrm{s} \quad . \end{aligned} \tag{14}$$

In the following, the determination of the corresponding energy capacities, especially with regard to the statement of minimization in (9), is presented.

Beforehand, a few auxiliary functions are introduced. First, the saturation function is needed, which limits the output of a function to a threshold value if this value is exceeded. Within this paper, it is defined symmetrically:

$$\mathrm{Sat}(p, P) = \begin{cases} P & p \geq P \\ p & -P < p < P \\ -P & p \leq -P \end{cases} \tag{15}$$

The residual of this function is defined by

$$\mathrm{ResSat}(p, P) = P - \mathrm{Sat}(p, P) \quad . \tag{16}$$

Further, a coordinate transformation is introduced:

$$\mathrm{Flip}(p(t), T) = -p(T - t) \tag{17}$$

This leads to a translation of the original coordinate system along the t-axis by T superposed by a 180° rotation.

At last, the following concept was developed to determine the energy capacity, referred to as Switched Decay Ordinary Differential Equation (SDODE) in the following:

$$\frac{\mathrm{d}e}{\mathrm{d}t} = \begin{cases} f^\mathrm{build}(t) & f^\mathrm{build} > 0 \\ f^\mathrm{decay}(t) & f^\mathrm{build} \leq 0 \ \wedge \ f^\mathrm{decay} < 0 \ \wedge \ e > 0 \\ 0 & \text{otherwise} \end{cases} \tag{18}$$

When solving this ODE, f^build gets integrated as long as this function is positive. When f^build is negative, f^decay is integrated instead, but only if f^decay by itself is negative and the integral e is larger than zero. The effect is that f^build always increases the value of e whereas f^decay always decreases this value, but never below zero.

To determine the required energy capacity E_p of the peak storage, the signal will be analyzed with the help of the SDODE in (18). The energy reserve of the peak storage that is needed to be available can be determined either by a charging event, i.e. positive peak signal parts, or by a discharging event, i.e. negative peak signal parts, where the peak storage must be adequately preloaded to be able to handle the demand. Therefore, positive and negative parts are treated separately and the SDODE will be utilized two times by defining differing f^build and f^decay functions:

1. For positive signal parts, the functions are set to

$$\begin{aligned} f^\mathrm{build}(t) &= \mathrm{ResSat}(p(t), P_\mathrm{b}) \\ f^\mathrm{decay}(t) &= \max(-P_\mathrm{p}, p^\mathrm{decay}(t)) \quad . \end{aligned} \tag{19}$$

   Depending on whether the control strategy allows an inter-storage power flow or not (see Section 2), the function p^decay is set to

$$\begin{aligned} p^\mathrm{decay,w/} &= p(t) - P_\mathrm{b} \qquad \text{or} \\ p^\mathrm{decay,w/o} &= p(t) \quad . \end{aligned} \tag{20}$$

   The build function in (19) ensures that only these signal parts are integrated that cannot be handled by the base storage. The decay function in (19) makes sure that the integral gets reduced again as fast as possible. The max-function guarantees that the power capacity P_p is not exceeded. If the control strategy allows a power flow between base and peak storages, the power capacity P_b of the base storage is placed at disposal in (20), otherwise the decay function is only composed of the signal $p(t)$.
2. For analyzing the negative part, build and decay functions are defined in the same way, but instead of the power $p(t)$, the flipped signal $p^\mathrm{rev}(t)$ is used with

$$p^\mathrm{rev}(t) = \mathrm{Flip}(p(t), T) \quad . \tag{21}$$

   This way, the signal is integrated backwards and future power demands can be anticipated.

Applying the SDODE in (18) for both positive and negative signal parts leads to the functions $e^+(t)$ and $e^-(t)$. To determine the minimal needed energy for the peak storage E_p, they are evaluated by

$$E_\mathrm{p} = \max\left(\max\left(e^+(t)\right), \max\left(e^-(t)\right)\right) \quad . \tag{22}$$

Then, the corresponding power for the base storage E_b can be determined with (4):

$$E_\mathrm{b} = E_\mathrm{s} - E_\mathrm{p} \tag{23}$$

Fig. 3 exemplarily shows the behaviour of the SDODE in (18) with the build and decay functions defined in (19) and (20). Fig. 3a shows the analyzed signal p as a function of time t,

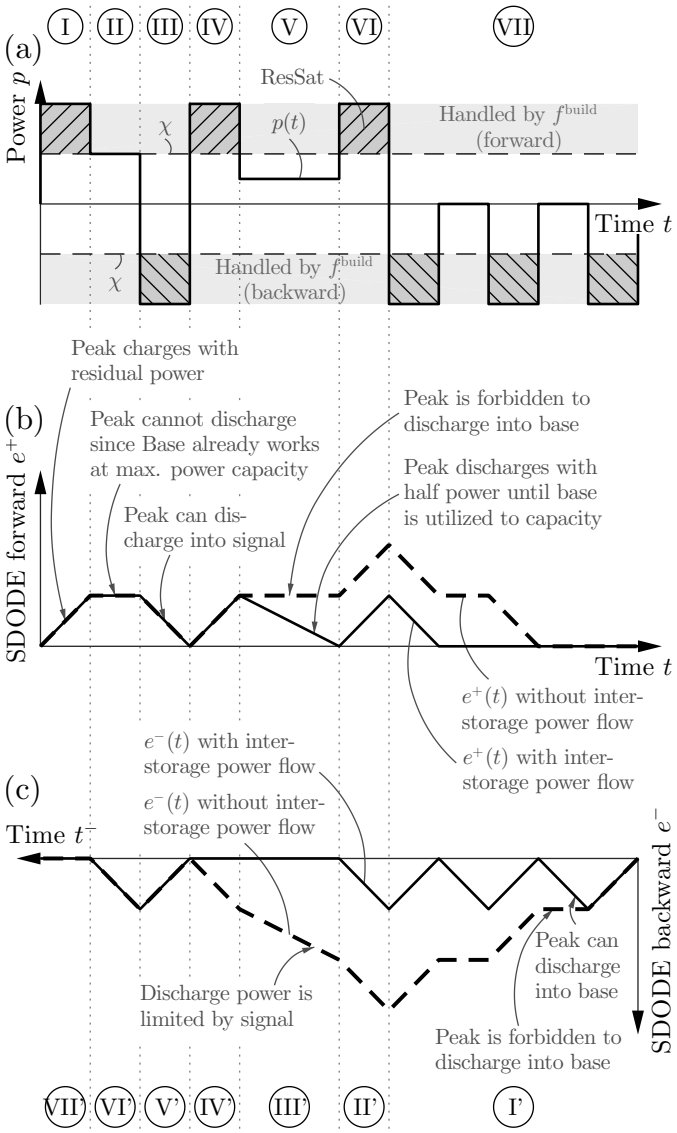

Figure 3: Example showing the principle of the SDODE in (18) for determining the minimal required peak energy capacity E_p. Fig. 3a shows the signal $p(t)$. The parts that are integrated by the build function f^{build} are shaded. Fig. 3b shows the integrated result of the SDODE. The solid line represents the result with an inter-storage power flow allowed, dashed line prohibited. Fig. 3c shows the results for the flipped signal p^{rev}.

which is chosen as a function with discrete steps to make the integration of that signal easily comprehensible. For further simplicity, a power cut $\chi = 0.5$ is chosen and the signal parts ResSat($p(t)$), which are handled by the peak storage, are shaded. All axes are dimensionless. Fig. 3b shows the SDODE $e^+(t)$ of $p(t)$ where the solid line represents the control strategy with inter-storage power flow and the dashed line without it. Fig. 3c shows the SDODE $e^-(t)$ of the reversed signal $p^{\text{rev}}(t)$. The diagram is adequately drawn in opposite direction since the signal is integrated backwards.

The result of the SDODE $e^+(t)$ in Fig. 3b is constructed as follows. In *Timeframe I*, the value of e^+ increases since $f^{\text{build}} = \text{ResSat}(p(t))$ is positive. In *Timeframe II*, f^{build} is zero, but f^{decay} is not lower than zero. Therefore, e^+ holds its value until it can decrease in *Timeframe III*, when f^{decay} gets negative for both control strategies. In *Timeframe IV*, the value of e^+ increases again. In the following *Timeframe V*, the curves for the different control strategies separate. While the decay function $f^{\text{decay}} = p(t) - P_\text{b}$ is negative for a control with allowed inter-storage power flow, $f^{\text{decay}} = p(t)$ is still positive for the latter case. Therefore, the solid line decreases again whereas the dashed line holds its value. In *Timeframe VI*, both lines increase again before they decrease in *Timeframe VII* in different time spans.

For the flipped SDODE $e^-(t)$, represented in Fig. 3c, the principle is identical. In *Timeframe I'*, the value of $e^-(t)$ increases and decreases within time in case of the control strategy with inter-storage power flow, as the peak storage is always able to discharge itself into the base storage. With a forbidden inter-storage power flow, the value increases but holds at those times where the signal $p^{\text{rev}}(t)$ is zero, as the peak storage is prohibited to discharge into base. In the subsequent timeframes, the value decreases again.

To determine the dimensions, the maximum values of e^+ and e^- must be determined according to (22). They are $E_{\text{p,w/}} = 1$ for an inter-storage power flow allowed and $E_{\text{p,w/o}} = 3$ for the latter case. The corresponding base storage energies evaluate with (23) to $E_{\text{b,w/}} = 7$ and $E_{\text{b,w/o}} = 5$. The needed single storage energy $E_\text{s} = 8$ can be calculated with (7).

3.4. Control Strategy

In the following, a control strategy is presented that proves the correctness of the dimensioning process. Depending on the structure or shape of the signal, there may be other control strategies that perform equally well in the sense that the power and energy capacities of the storages are not exceeded in some point in time by simultaneously handling the complete requirement of the signal. The presented one will work for any signal at the expense that it generally needs the signal information in advance by utilizing the flipped SDODE result $e^-(t)$ obtained from the previous dimensioning process.

The control strategy is represented in a block diagram in Fig. 4 and can be mathematically expressed by the following set of differential and algebraic equations. It is explained afterwards.

$$\begin{pmatrix} p_\text{b} \\ p_\text{p} \end{pmatrix} = \begin{cases} \text{ReloadMode}(p, e_\text{p}) & \tau_\text{p} < \tau_\text{b} \\ \text{SyncMode}(p) & \tau_\text{p} \geq \tau_\text{b} \end{cases} \tag{24}$$

With τ_i:

$$\tau_i = \begin{cases} \frac{E_i - e_i(t)}{P_i} & e_\text{p}(t) > e^{\text{BW}}(t) \\ \frac{e_i(t)}{P_i} & e_\text{p}(t) \leq e^{\text{BW}}(t) \end{cases} \quad \text{with} \quad i \in \{\text{b}, \text{p}\} \tag{25}$$

Variable e^{BW} denotes the backward integral obtained from the SDODE e^-:

$$e^{\text{BW}}(t) = -\text{Flip}(e^-(t), T) \tag{26}$$

The utilisation of e^{BW} can be interpreted as a look into the future, which may complicate the implementation of this control strategy in reality. The ReloadMode() is defined by

$$\begin{pmatrix} p_\text{b}(t) \\ p_\text{p}(t) \end{pmatrix} = \begin{pmatrix} \text{Sat}(p(t) + p^{\text{req}}(t)) \\ p(t) - p_\text{b}(t) \end{pmatrix} \tag{27}$$

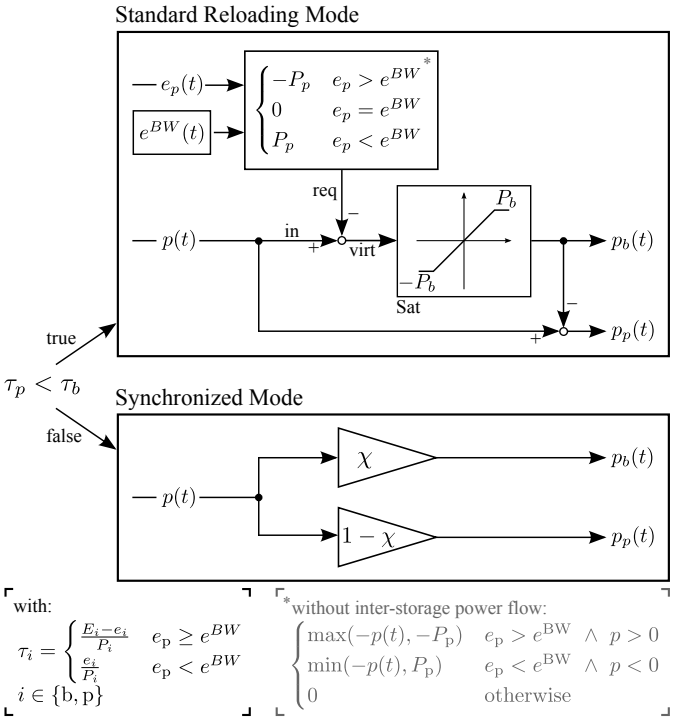

Figure 4: Control Strategy Block Diagram; Standard Reloading Mode that ensures a minimum usage of peak storage. Peak storage requests discharging power; whether it actually can do it, depends on instantaneous input power. The storage system will switch to Synchronized Mode when base and peak storages are both nearly full to prevent the base storage getting full prematurely.

and the SyncMode() by

$$\begin{pmatrix} p_\mathrm{b}(t) \\ p_\mathrm{p}(t) \end{pmatrix} = \begin{pmatrix} \chi \cdot p(t) \\ (1-\chi) \cdot p(t) \end{pmatrix} \quad . \tag{28}$$

The requested power p^{req} varies depending on whether an inter-storage power flow is allowed or not. For the first case it is

$$p^{\mathrm{req,w/}} = \begin{cases} -P_\mathrm{p} & e_\mathrm{p} > e^{\mathrm{BW}} \\ 0 & e_\mathrm{p} = e^{\mathrm{BW}} \\ P_\mathrm{p} & e_\mathrm{p} < e^{\mathrm{BW}} \end{cases} \tag{29}$$

and for the latter one it is

$$p^{\mathrm{req,w/o}} = \begin{cases} \max(-p(t), -P_\mathrm{p}) & e_\mathrm{p} > e^{\mathrm{BW}} \ \wedge \ p > 0 \\ \min(-p(t), P_\mathrm{p}) & e_\mathrm{p} < e^{\mathrm{BW}} \ \wedge \ p < 0 \\ 0 & \text{otherwise} \end{cases} \quad . \tag{30}$$

The control strategy consists of a Standard Reloading Mode and a Synchronized Mode that will be switched depending on the State Of Charge of the base and peak storages. For now, the explanation of the switching condition is deferred. First, assume the Standard Reloading Mode is active. In this mode, the peak storage requests a positive or negative power p^{req} depending on its current State Of Charge and the aimed State Of Charge (cp. Fig. 4). Whether it actually can charge or discharge depends on the input power p. The input power p is superposed with the requested power p^{req}, building a virtual power p^{virt}. The base storage supplies as much power as possible holding the limitations in (8) and the residual power is supplied by the peak storage.

The aimed stored energy of the peak storage, which determines the requested power, is generally zero. This satisfies the requirement that the peak storage shall provide not more energy than needed. Nevertheless, this strategy would fail if a high negative power is demanded that cannot be handled by the base storage alone. Then, the peak storage needs to be precharged in advance and the aimed energy content switches to E_p. These precharging events can be detected with the help of the negative SDODE $e^{-}(t)$ determined during dimensioning. It is transformed back into the original coordinate system, gaining the backward integral e^{BW}. If the peak storage energy $e_\mathrm{p}(t)$ is lower than $e^{\mathrm{BW}}(t)$, the peak storage will switch into charging mode, requesting the power P_p.

In Synchronized Mode, the input power p is evenly distributed with respect to χ, so the base storage will supply $\chi \cdot p$ of the power, and the peak storage $(1-\chi) \cdot p$ of the power. This guarantees that both storages get completely charged at the same time, which is needed at the end of a charging phase. Suppose both storages are nearly completely charged. Without synchronizing the storages, the peak storage will continue to discharge itself into the base storage, which will lead to a situation where the base storage gets prematurely fully charged and cannot take power anymore.

To detect the required switch from Reloading Mode to Synchronized Mode, the times τ_p and τ_b are introduced. These are the times that would be needed to completely charge the individual storages with their maximum powers from the current State Of Charge, or to completely discharge if the peak storage is currently in charging mode. When the time τ_b gets lower than τ_p, the control strategy switches to Synchronized Mode.

An example demonstrating the control strategy is provided in Fig. 5. Fig. 5a shows the input power as a solid line and the base and peak powers as shaded areas. The power cut $\chi = 0.4$ is marked as a dashed line. Fig. 5b shows the State Of Charge of both storages as a solid line, and the normalized backward integral $e^{\mathrm{BW}}/E_\mathrm{p}$ as a dashed line.

In *Timeframe I*, the input power $p(t)$ is taken by the base storage as long as it is below its maximum power. When $p(t)$ exceeds this value, the peak storage takes the residual power. Right at this moment, the peak storage already requests to discharge again but cannot until *Timeframe II*. Here, the base storage continues to charge with its maximum power to meet the discharging request of the peak storage in the best possible way. In *Timeframe III*, the peak storage is empty again and the base storage switches back supplying the input power $p(t)$. *Timeframe IV* completely charges the peak storage, which will discharge in *Timeframe V*, again. At the beginning of *Timeframe VI*, the peak storage stops to discharge with maximum power and switches to a charging request because the backward integral e^{BW} indicates that the remaining energy of the peak storage is needed to supply the discharge event. *Timeframe VII* charges the base storage again. In *Timeframe VIII*, the storage system switches to Synchronized Mode. Otherwise, the base storage would be prematurely full and cannot provide power anymore at the end of the charging cycle.

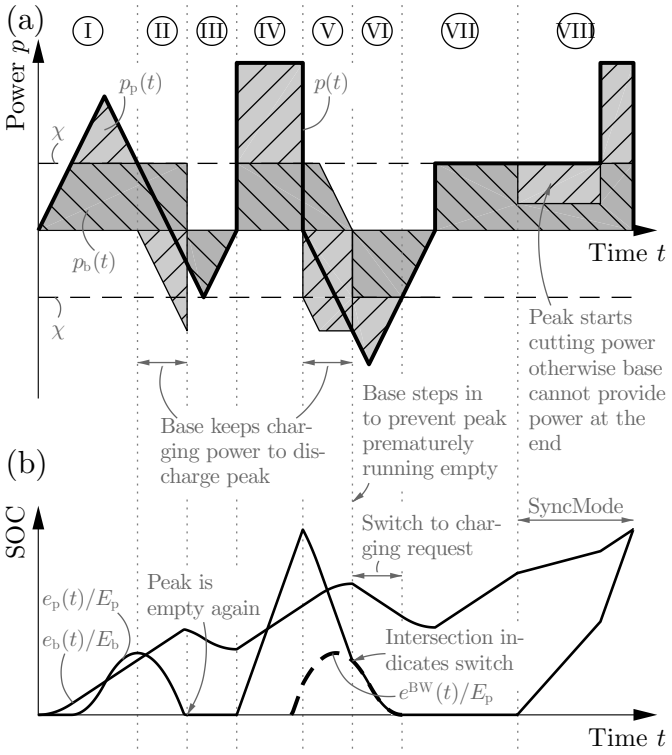

Figure 5: Exemplary demonstration of the control strategy, showing the charging phase of a signal. Fig. 5a shows powers, Fig. 5b shows State Of Charge. Various states and modes like charging request, discharging request, or Synchronized Mode are indicated.

4. Technology Selection

Next, it is demonstrated how the Hybridisation Diagram, derived from the previous elaborations, can be used to select a specific storage pairing of base and peak storages from available storage technologies. The enclosed area *(I)* in the Hybridisation Diagram in Fig. 1 indicates all possible or allowed storage tuples with an infinite amount of different specific powers. In reality, it can only be chosen from a finite set of different storage technologies with distinct specific powers. So, for an arbitrarily chosen specific power cut χ, the corresponding tuple of base and peak storages must be mapped to the available technologies. This generally leads to overdimensioning and is furtherly advanced in Fig. 6 and the next paragraphs.

The Hybridisation Diagram, which is introduced in Fig. 1, is complemented in Fig. 6 by the specific power lines of available technologies. All technologies with a specific power lower than the specific power of the single storage system are represented in the lower left base storage coordinate system. Technologies with a higher specific power are represented in the upper right peak storage coordinate system. In Fig. 6a to Fig. 6e, a base and a peak storage technology are arbitrarily chosen in a way that the intersection point of the two technology lines is within the Hybridisation Area. In Fig. 6f, the technologies are chosen in a way that the intersection point is outside.

In Fig. 6a, the HESS operates at a power cut χ_{I}, which is exactly at the height of the intersection point of the two storage technologies. The dimensions of the base and peak storages are indicated as grey hatched rectangles in their corresponding coordinate system. At this point, the hybrid storage system is neither overdimensioned in energy nor in power. This can be seen as the two rectangles only touch each other in their corner. For other power cuts $\chi \neq \chi_{\mathrm{I}}$, the rectangles will overlap and the hybrid storage system will be overdimensioned, as it can be seen in the following.

In Fig. 6b, a power cut $\chi_{\mathrm{II}} > \chi_{\mathrm{I}}$ is chosen. Then, the power cut intersects with the storage technology lines at two different points. To find an adequate storage pairing, select the intersection point of the power cut with the base storage technology line. The tuple of base and peak storages in this point cannot be realized as the base storage technology line crosses this point, but the peak storage technology line does not. The corresponding peak storage must have at least the amount of energy and power but it must also be on the peak storage technology line. Therefore, a horizontal mapping to the peak storage technology line is required as indicated by the arrow in Fig. 6b. The result is that the system will be overdimensioned in energy by the length of the arrow, but not in power. The edges of the rectangles, which represent the dimensions of the base and peak storages, now overlap to some extend. Note, that this extra amount of energy capacity will not be utilised by the peak storage during operation and that the whole HESS behaves as the storage tuple in the first chosen point. This mapping can also be done by starting at the peak storage technology line, but the result with regard to the overdimensioning will be the same in this case.

The construction for power cuts $\chi_{\mathrm{III}} < \chi_{\mathrm{I}}$ follows the same principles but leads to a pareto front of minimal solutions, as it can be seen in the following in Fig. 6c and Fig. 6d. Again, the power cut intersects the technology lines of base and peak storages. If the intersection point with the base storage technology line is chosen (cp. Fig. 6c), the peak storage technology line does not cross this point. A peak storage with at least the corresponding energy and power capacities can be found by vertically mapping downwards to the peak storage technology line. Remember, the peak storage coordinate system is rotated, hence moving downwards is equal to additional power capacity. In this case, the HESS is overdimensioned in power by the length of the arrow (cp. Fig. 6c), but not in energy. Again, this extra amount of power capacity will not be utilised in operation and the HESS behaves as the tuple chosen where the power cut intersects with the base storage technology line. The construction can also be done by starting at the intersection of the power cut and the peak storage (cp. Fig. 6d). Then, the mapping from the peak storage to the smallest allowed base storage is done by moving vertically upwards to the base storage technology line. This will yield another pairing which is overdimensioned in power but not in energy. Again, the HESS will behave in operation as the tuple where the construction started. Also, all variations in between those two pairings are possible, leading, as mentioned above, to a pareto front of minimal solutions. Generally, the pair in Fig. 6d will be the preferred one for power cut χ_{III} as long as the specific costs per energy of the base storage are smaller than the specific costs per energy of peak storage.

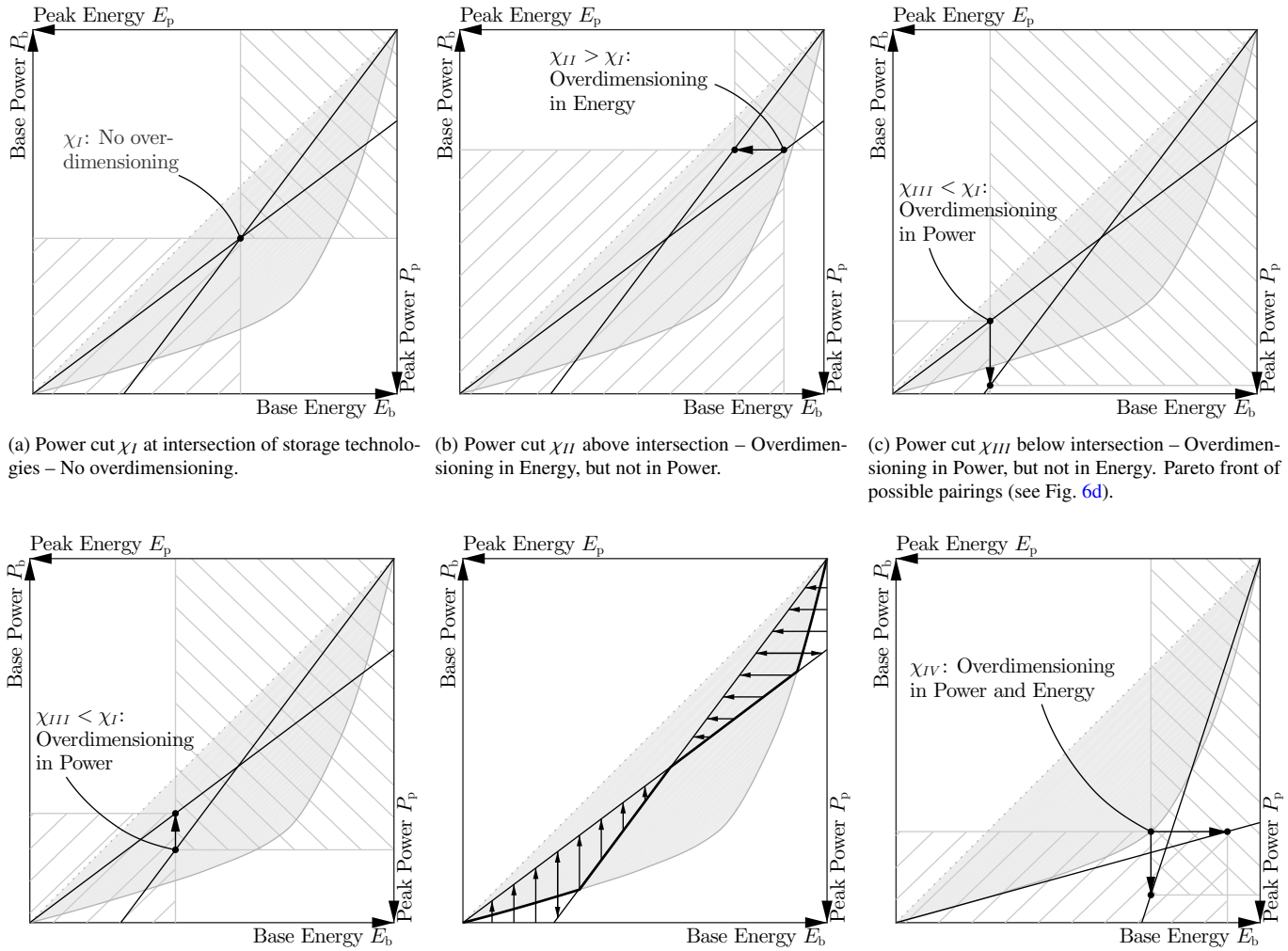

(a) Power cut χ_I at intersection of storage technologies – No overdimensioning.

(b) Power cut χ_{II} above intersection – Overdimensioning in Energy, but not in Power.

(c) Power cut χ_{III} below intersection – Overdimensioning in Power, but not in Energy. Pareto front of possible pairings (see Fig. 6d).

(d) Identical power cut χ_{III} below intersection – Second alternative, generally preferred since overdimensioning is smaller (cp. to Fig. 6c).

(e) Summary of previous elaborations. Storage pairings as a function of the power cut (thick black line).

(f) Mapping if intersection of storages is outside Hybridisation Area – Overdimensioning in both energy and power.

Figure 6: Concrete selection of a storage pairing from two specific storage technologies will generally lead to overdimensioning. Depending on the chosen power cut at which the storages shall operate, the system may be overdimensioned in power, in energy or both.

The former elaborations are unified in Fig. 6e. Here, the storage pairs are depicted as a function of the power cut χ (thick black line). From this line, the base and peak storages are found by mapping along the arrows. Note that for low and high power cuts χ, one of them might be outside the diagram. Moreover, if one of the technology lines is outside the Hybridisation Area, the construction is started at the Hybridisation Line. Then, the mapping must be performed to both base and peak storages.

Last, a second technology pairing is examined in Fig. 6f. The intersection of base storage specific power line and peak storage specific power line is outside the Hybridisation Area. In this case, the corresponding tuple of base and peak storages cannot be realized as in the case that is shown in Fig. 6a. To find the minimal *Pairing IV* for a power cut χ_IV, where both base and peak specific power lines are outside the Hybridisation Area, map from the intersection point of the power cut χ_IV with the Hybridisation Curve to the base storage specific power line along a horizontal line and to the peak storage specific power line along a vertical line. The resulting storage pair will be overdimensioned in both energy and power.

Summarizing, for two distinct storage technologies, there is at most one point or power cut χ at the intersection of these two technologies, where the system is not overdimensioned. For power cuts below this intersection, the system will be overdimensioned in power; for power cuts above the intersection, the system will be overdimensioned in energy. If the specific power lines of base and peak storages are both outside the Hybridisation Area, the system will be overdimensioned in both power and energy. Again, the additionally allocated power and energy capacities will not be used in operation and the HESS will act as the tuple at the hybridisation line.

The previously described mapping can also be expressed mathematically, which will be presented in the following. After some minimizations of logical expressions, the following set of equations can be obtained to determine the optimal pairing for

Table 1: Storage Technology Paramters [16]

	Technology	Spec. Power kW/kWh	Spec. Costs EUR/kWh	Spec. Weight kg/kWh
Pb	Lead Acid	2	350	40
LiPo	Lithium Polymer	4	600	9
FW	Flywheel	15	2000	100
SC	Super Capacitor	40	5200	1000

a certain power cut χ:

$$\chi \mapsto (E_\mathrm{b}^*, E_\mathrm{p}^*, E_\mathrm{h}^*) \tag{31}$$

Here, the index h denotes the Hybridisation Curve, and the asterisk * denotes the intersection point of the power cut χ with the separate lines. The intersection points are all evaluated in base coordinate system. Then, the energy capacities of base and peak storages are determined by:

$$\begin{aligned} E_\mathrm{b} &= \begin{cases} \min(E_\mathrm{p}^*, E_\mathrm{h}^*) & E_\mathrm{b}^* < \min(E_\mathrm{p}^*, E_\mathrm{h}^*) \\ E_\mathrm{b}^* & \text{otherwise} \end{cases} \\ E_\mathrm{p} &= \min(E_\mathrm{p}^*, E_\mathrm{h}^*) \end{aligned} \tag{32}$$

With the known energy capacities, the power capacities can be mapped easily:

$$\begin{aligned} E_\mathrm{b} &\mapsto P_\mathrm{b} \\ E_\mathrm{p} &\mapsto P_\mathrm{p} \end{aligned} \tag{33}$$

This set of equations can be used for an automated investigation of the problem.

5. Examples

In this section, two examples or applications shall be discussed. First, a pulsed load as a rather academic example is investigated. Second, storage system configurations for a driving cycle shall be analyzed. For both examples, the parameters in Table 1 were used. They are purposely chosen in a way to produce visual rich results and diagrams, not to obtain quantitatively applicable data. Instead, the focus is on demonstrating the methodology. The parameters are obtained from [16] from specified ranges.

5.1. Pulsed Loads

Pulsed loads are thoroughly investigated in the context of HESS or battery-supercapacitor combinations in analytical, numerical and experimental form [4, 5, 17, 18, 19, 20]. Studies are performed for passive topologies as well as semi-active and active topologies in both time and frequency domain. The aim is to reduce the dynamic stress of the battery to extend its lifetime or to reduce costs and battery size. The outcome largely depends on the definitions of the signal in terms of pulse rate θ, which defines the time until a pulse is repeated, and pulse duty ratio θ^*/θ, which defines the width of a pulse (cp. inset of Fig. 7a) [19].

This study analyzes a pulsed signal with respect to its specific power and the potential of using different storages with different specific powers that can be combined to an HESS to meet the one of the signal. In this case, a signal with 100 repetitive 1 MW-pulses, a pulse rate of $\theta = 60\,\mathrm{s}$ and a duty ratio of $\theta^*/\theta = 1/10$ is chosen. The energy content of that signal is 166.7 kWh. Note, that only the charging phase is analyzed, and it is not of interest how the HESS is discharged again. Therefore, the discharging phase is virtually point-mirrored to fulfil (11) without modifying the outcome. Lead-Acid (*Pb*) and Lithium Polymer (*LiPo*) batteries as base storage, and Super Capacitors (*SC*) as peak storage (cp. Table 1) are subject of investigation. If the signal shall be solved with a Pb-battery alone, one would need to install 500 kWh at costs of 175 000 EUR in order to handle a 1 MW peak power pulse. Comparing this to the theoretically needed energy capacity, two thirds of the energy capacity of the Pb-battery would be unused. In case of the LiPo-battery, still, 250 kWh at costs of 150 000 EUR need to be installed to meet the power demand. On the other hand, when using a SC for the application, one would need to install a power capacity 6.7 MW at costs of 833 000 EUR to meet the energy demand.

The accomplishable results with the help of the proposed hybridisation method are shown in Fig. 7. Fig. 7a is structured in the same manner as Fig. 6e. Fig. 7b supplements the former one by the costs of the HESS as a function of the power cut χ. There are now two possible technology pairings: *Pb-SC* and *LiPo-SC*. The cost curve of pairing *Pb-SC* is drawn as a dashed line and for pairing *LiPo-SC* as dash-dotted line. Both of them have a minimum at the intersection point of the technology lines in Fig. 7a (at $\chi = 0.3$ and $\chi = 0.63$) and increase linearly above and below this power cut χ (A simple linear cost model is assumed in this paper, where the costs of a storage linearily scale with its energy content (cp. Table 1)). At $\chi = 0.53$, both pairings have equal costs. Below this power cut χ, *Pb-SC* has lower costs, above this power cut, *LiPo-SC* has lower costs. The resulting minimum cost curve considering all pairings is drawn as a solid line in Fig. 7b. The solid black power cut line in Fig. 7a is only drawn for the storage pairing with the lowest costs. Therefore, it has a discontinuity at $\chi = 0.53$ and switches from pairing *Pb-SC* to pairing *LiPo-SC*.

It can be observed by the shaded Hybridisation Area that the signal has a high Hybridisation Potential of $H = 0.9$. The Reloading Potential is $R = 0.9$, as well. This means that hybridisation is only possible through an inter-storage power flow. The intersections of both *Pb*- and *LiPo*-technology lines with the *SC*-technology line are inside the Hybridisation Area. Following, a storage tuple exists for both pairings that is not overdimensioned.

For *Pairing Pb-SC*, this point is at $\chi = 0.3$. Then, the storages have the following dimensions:

$$\chi = 0.3 \quad \mapsto \quad \begin{pmatrix} P_\mathrm{b,Pb} = 300\,\mathrm{kW} & E_\mathrm{b,Pb} = 150\,\mathrm{kWh} \\ P_\mathrm{p,SC} = 700\,\mathrm{kW} & E_\mathrm{p,SC} = 16.7\,\mathrm{kWh} \end{pmatrix}$$

The *Pairing LiPo-Sc* intersects at power cut $\chi = 0.63$ which

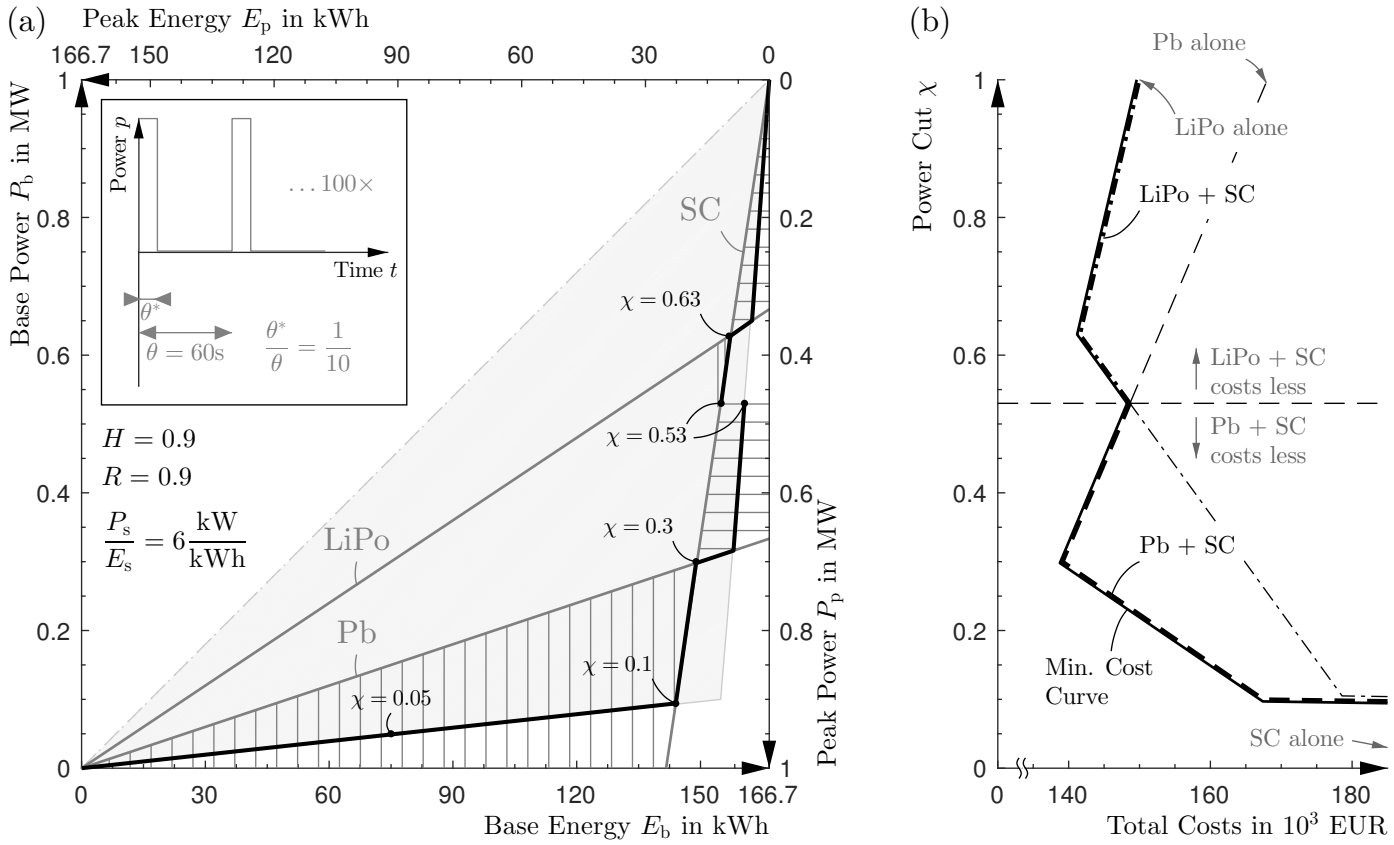

Figure 7: Hybridisation Diagram for a Pulsed Load complemented by specific power lines of *Pb*, *LiPo* and *SC* technologies (grey lines). The black line indicates, in conjunction with the thin vertical and horizontal lines, the optimal pairing as a function of power cut χ. Below power cut $\chi = 0.53$, *Pb-SC*–combinations are preferred, above *LiPo-SC*–combinations. Optimal pairings with minimal costs are at the intersection points $\chi = 0.3$ and $\chi = 0.63$.

results in

$$\chi = 0.63 \quad \mapsto \quad \begin{pmatrix} P_{b,LiPo} = 630\,kW & E_{b,LiPo} = 158\,kWh \\ P_{p,SC} = 370\,kW & E_{p,SC} = 8.7\,kWh \end{pmatrix} .$$

As it can be seen in Fig. 7b, both technology pairings have investment costs of approximately 140 000 EUR. Concluding, none of them is preferred from this point of view.

This analysis does only consider installation costs, but not operating costs or replacement costs. Also, the analyzed system does not have any losses. Additional power and energy capacities would be needed to take them into account. Moreover, the methodology does not inherently increase the system response time or reduce the dynamic stress on the battery. This may only happen as a side effect (which actually occurs in this example as the battery will be steadily charged while the SC takes care of the peaks), but this is not guaranteed. Further analysis or simulations should address this issue, e.g. by superposing the control strategy of this analysis with a filtration-based control (e.g. [1, 7, 21]).

Technology parameter variations can be easily analyzed graphically in Fig. 7. Higher specific powers ω would tilt the technology lines counter-clockwise, lower specific powers clockwise. For example, a lower specific power $\omega_{b,Pb}$ of *Pb* would lead to an intersection with *SC* at a lower power cut χ, varying the single dimensions of *Pairing Pb-SC*. A specific power $\omega_{p,SC}$ that is 3 or 4 times higher than the current value would have the effect that the intersections with the base technology lines are outside the Hybridisation Area, with the consequence that there is no longer a storage tuple that is not overdimensioned.

5.2. Artemis Driving Cycle

Storage hybridisation is largely considered for the electrification of vehicles since an effective usage of the storage is crucial for minimizing costs, weight and enhancing lifetime [8, 9, 10, 12, 13, 14, 15, 18, 21, 22, 23]. Investigations are performed with different driving cycles, models and parameters assumed, making it hard to produce consistent and comparable results. In this paper, a driving cycle derived from data of the Artemis project is analyzed [24]. To obtain reasonable results, the urban, rural, and highway driving cycles are concatenated two times to achieve a total distance of 101 km. Then, the required power is calculated by the following vehicle model derived from [18] with the parameter set in Table 2.

$$p(t) = \frac{1}{\eta}\left(m \cdot \frac{dv}{dt} + mgc_r + \frac{1}{2}\rho A c_d \cdot v^2\right) \cdot v \qquad (34)$$

Since only qualitative results are desired, this simple model will be sufficient. As only the discharging phase is of interest, the

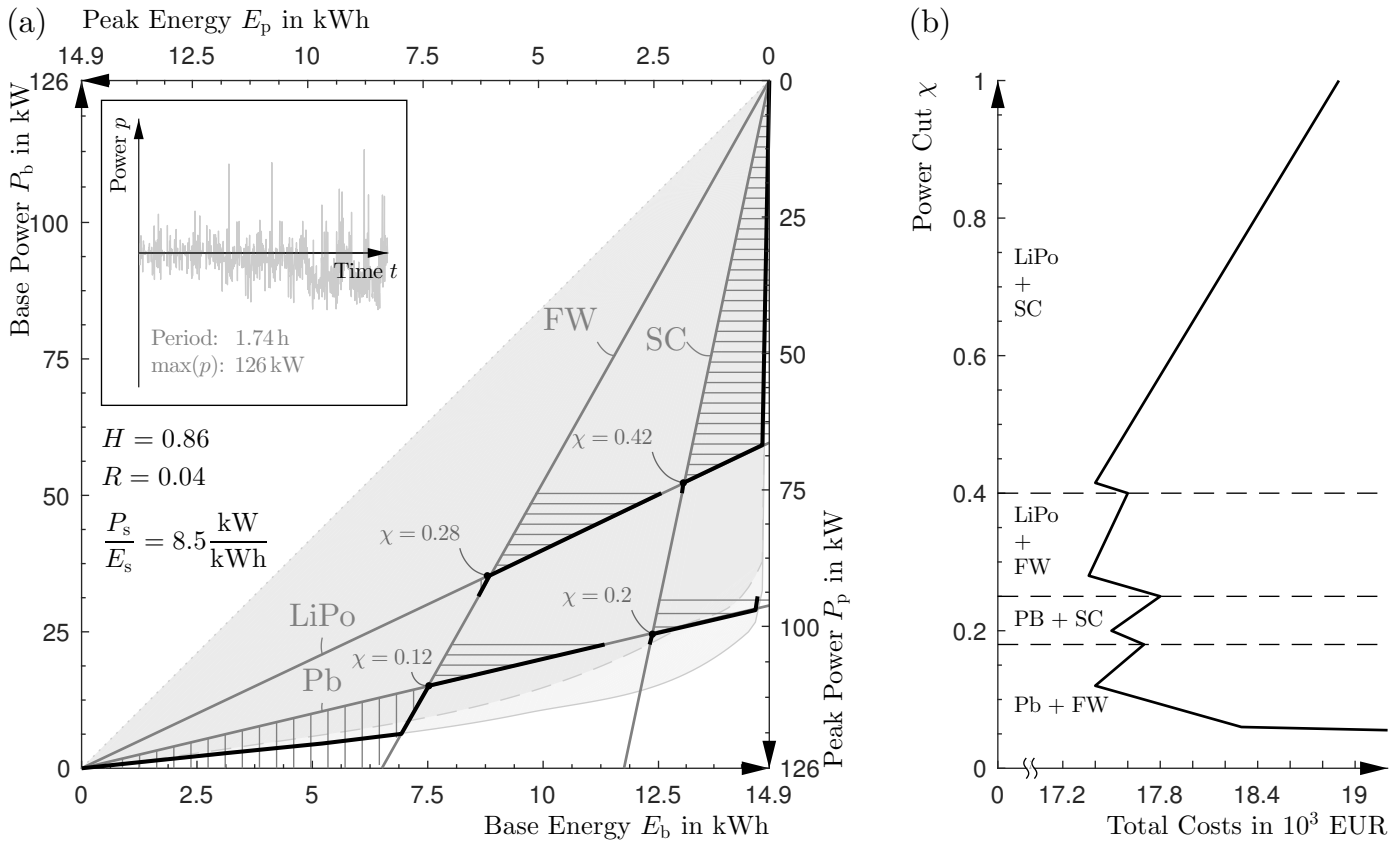

Figure 8: Hybridisation Diagram for a concatenated Artemis Driving Cycle (2× (Urban + Rural + Highway) = ∑ 101 km) complemented by technology selection information for *Pb*, *LiPo*, *FW* and *SC* technologies. All intersections are within the Hybridisation Area. Following, a minimal dimensioning solution can be potentially chosen for all combinations at different power cuts χ.

Table 2: Vehicle model parameters

Parameter Name	Variable	Value	Unit
Total reduced mass with storage	m	1400	kg
Effective frontal area of vehicle	A	2.25	m^2
Rolling resistance coefficient	c_r	0.01	
Aerodynamic drag coefficient	c_d	0.3	
Total power train efficiency	η	0.8	
Gravitational acceleration	g	9.81	m/s^2
Density of air	ρ	1.29	kg/m^3

signal is point mirrored for the same reasons as in the previous example.

The results shown in Fig. 8 are structured in the same manner as in Fig. 7. Additionally, Flywheel-technology (*FW*) (cp. Table 1) is also considered as a potential peak storage beside the previously introduced technologies. Hence, there are now four potential technology pairings: *Pb-FW*, *Pb-SC*, *LiPo-FW* and *LiPo-SC*. For this reason, the information in the Hybridisation Diagram is denser but the principles to read the diagram are the same. In Fig. 8b, only the minimum cost curve is drawn for the respective technology pairing for each section as illustrating all separate cost curves would add too much information to the diagram.

Although the required energy and power capacities E_s and P_s for the driving cycle have a by one decade lower magnitude compared to the pulsed load, Fig. 7 and Fig. 8 look quite similar because the specific power of the single storage $\omega_s = 8.2$ kW/kWh and the Hybridisation Potential $H = 0.86$ of the driving cycle differ only slightly.

Again, all intersections of the technology lines are within the Hybridisation Area, leading to 4 minimal pairings at $\chi = 0.11$ for *Pairing Pb-FW*, at $\chi = 0.2$ for *Pairing Pb-SC*, at $\chi = 0.27$ for *Pairing LiPo-FW* and at $\chi = 0.42$ for *Pairing LiPo-SC*. The estimated costs for all pairings are approximately 17 400 EUR, so a beneficial pairing cannot be chosen with the available data. A selection has to be found through further considerations. Since a low weight is of high importance, combinations with *Pb* can be discarded (cp. Table 1), but a combination of *LiPo* with *FW* or *SC* is worth investigating. Again, the same limitations as described in the previous example apply to this one. This analysis only tunes the specific power of the HESS. Further capacity is needed due to losses, operation and replacement costs must be addressed and parameters such as system response time or dynamic stress must be investigated in subsequent analysis.

6. Conclusion and Summary

The paper introduces the analytical and theoretical concept to calculate a minimal set of storage pairings for a specific signal/problem in a sense that the added power and energy capacities of both storages equal the capacities of an equivalent single

storage. Additionally, for this set of storages, the energy of one of them becomes minimal. To describe the results, integral Hybridisation Parameters are provided as well as a visualization in form of the Hybridisation Diagram. It is shown that any single storage system can be split into an HESS and that the potential or effectiveness of this hybridisation is signal dependent. The results are accompanied by the mathematical and modelling background, as well as a control strategy as proof. An economic choosing strategy for specific technologies expands the base theory.

Exemplarily, the theory was applied to a pulsed periodic load and a driving scenario. As already demonstrated in other studies, this work confirms that a beneficial combination of batteries with supercapacitors or other storage types is feasible.

The main drawback of the theory is its theoretical nature, which reduces the problem to an energy balance and requires an omniscient control strategy. Therefore, it only serves as a predimensioning and preselection tool, as well as potential analysis for hybridisation of a signal. It can easily be determined if an application is suitable for hybridisation and benefical storage combinations can be derived including its dimensions. In future work, a storage model considering losses will be implemented but the theory will keep its status to be only a pre-dimensioning tool. Instead, it is aimed towards a universal methodology that defines the neglected subsequent steps needed for a comprehensive system design in a generally applicable manner.

A toolbox is provided at https://github.com/s-guenther/hybrid.git and the reader is encouraged to use or expand it for her/his own work. Further information, details and documentation can be found there.

[1] L. W. Chong, Y. W. Wong, R. K. Rajkumar, R. K. Rajkumar, D. Isa, Hybrid energy storage systems and control strategies for stand-alone renewable energy power systems, Renewable and Sustainable Energy Reviews 66 (2016) 174–189. doi:10.1016/j.rser.2016.07.059.

[2] R. Hemmati, H. Saboori, Emergence of hybrid energy storage systems in renewable energy and transport applications – A review, Renewable and Sustainable Energy Reviews 65 (2016) 11–23. doi:10.1016/j.rser.2016.06.029.

[3] T. Bocklisch, Hybrid energy storage systems for renewable energy applications, Energy Procedia 73 (Supplement C) (2015) 103 – 111, 9th International Renewable Energy Storage Conference, IRES 2015. doi:https://doi.org/10.1016/j.egypro.2015.07.582.

[4] A. Kuperman, I. Aharon, Battery–ultracapacitor hybrids for pulsed current loads: A review, Renewable and Sustainable Energy Reviews 15 (2) (2011) 981–992. doi:10.1016/j.rser.2010.11.010.

[5] A. Lahyani, A. Sari, I. Lahbib, P. Venet, Optimal hybridization and amortized cost study of battery/supercapacitors system under pulsed loads, Journal of Energy Storage 6 (2016) 222–231. doi:10.1016/j.est.2016.01.007.

[6] Y. Zhang, X. Tang, Z. Qi, Z. Liu, The Ragone plots guided sizing of hybrid storage system for taming the wind power, International Journal of Electrical Power & Energy Systems 65 (2015) 246–253. doi:10.1016/j.ijepes.2014.10.006.

[7] D. B. W. Abeywardana, B. Hredzak, V. G. Agelidis, G. D. Demetriades, Supercapacitor Sizing Method for Energy-Controlled Filter-Based Hybrid Energy Storage Systems, IEEE Transactions on Power Electronics 32 (2) (2017) 1626–1637. doi:10.1109/TPEL.2016.2552198.

[8] E. Schaltz, A. Khaligh, P. O. Rasmussen, Influence of Battery/Ultracapacitor Energy-Storage Sizing on Battery Lifetime in a Fuel Cell Hybrid Electric Vehicle, IEEE Transactions on Vehicular Technology 58 (8) (2009) 3882–3891. doi:10.1109/TVT.2009.2027909.

[9] J. Shen, S. Dusmez, A. Khaligh, Optimization of Sizing and Battery Cycle Life in Battery/Ultracapacitor Hybrid Energy Storage Systems for Electric Vehicle Applications, IEEE Transactions on Industrial Informatics 10 (4) (2014) 2112–2121. doi:10.1109/TII.2014.2334233.

[10] J. Shen, A. Hasanzadeh, A. Khaligh, Optimal power split and sizing of hybrid energy storage system for electric vehicles, in: IEEE Transportation Electrification Conference and Expo (ITEC), 2014, IEEE, Piscataway, NJ, 2014, pp. 1–6. doi:10.1109/ITEC.2014.6861861.

[11] A. M. Abd-el Motaleb, S. K. Bekdach, Optimal sizing of distributed generation considering uncertainties in a hybrid power system, International Journal of Electrical Power & Energy Systems 82 (2016) 179–188. doi:10.1016/j.ijepes.2016.03.023.

[12] M. Masih-Tehrani, M.-R. Ha'iri-Yazdi, V. Esfahanian, A. Safaei, Optimum sizing and optimum energy management of a hybrid energy storage system for lithium battery life improvement, Journal of Power Sources 244 (2013) 2–10. doi:10.1016/j.jpowsour.2013.04.154.

[13] M.-E. Choi, J.-S. Lee, S.-W. Seo, Real-Time Optimization for Power Management Systems of a Battery/Supercapacitor Hybrid Energy Storage System in Electric Vehicles, IEEE Transactions on Vehicular Technology 63 (8) (2014) 3600–3611. doi:10.1109/TVT.2014.2305593.

[14] R. E. Araujo, R. de Castro, C. Pinto, P. Melo, D. Freitas, Combined Sizing and Energy Management in EVs With Batteries and Supercapacitors, IEEE Transactions on Vehicular Technology 63 (7) (2014) 3062–3076. doi:10.1109/TVT.2014.2318275.

[15] Z. Song, H. Hofmann, J. Li, X. Han, X. Zhang, M. Ouyang, A comparison study of different semi-active hybrid energy storage system topologies for electric vehicles, Journal of Power Sources 274 (2015) 400–411. doi:10.1016/j.jpowsour.2014.10.061.

[16] M. Sterner, I. Stadler, Energiespeicher - Bedarf, Technologien, Integration, SpringerLink : Bücher, Springer Vieweg, Berlin, 2014.

[17] T. Ma, H. Yang, L. Lu, Development of hybrid battery–supercapacitor energy storage for remote area renewable energy systems, Applied Energy 153 (2015) 56–62. doi:10.1016/j.apenergy.2014.12.008.

[18] C. Zhao, H. Yin, Z. Yang, C. Ma, A quantitative comparative study of efficiency for battery-ultracapacitor hybrid systems, IECON Proceedings (Industrial Electronics Conference)doi:10.1109/IECON.2014.7048949.

[19] R. A. Dougal, S. Liu, R. E. White, Power and life extension of battery-ultracapacitor hybrids, IEEE Transactions on Components and Packaging Technologies 25 (1) (2002) 120–131. doi:10.1109/6144.991184.

[20] L. Gao, R. A. Dougal, S. Liu, Power Enhancement of an Actively Controlled Battery/Ultracapacitor Hybrid, IEEE Transactions on Power Electronics 20 (1) (2005) 236–243. doi:10.1109/TPEL.2004.839784.

[21] S. Dusmez, A. Khaligh, A Supervisory Power-Splitting Approach for a New Ultracapacitor–Battery Vehicle Deploying Two Propulsion Machines, IEEE Transactions on Industrial Informatics 10 (3) (2014) 1960–1971. doi:10.1109/TII.2014.2299237.

[22] J. Shen, A. Khaligh, A Supervisory Energy Management Control Strategy in a Battery/Ultracapacitor Hybrid Energy Storage System, IEEE Transactions on Transportation Electrification 1 (3) (2015) 223–231. doi:10.1109/TTE.2015.2464690.

[23] J. Cao, A. Emadi, A New Battery/UltraCapacitor Hybrid Energy Storage System for Electric, Hybrid, and Plug-In Hybrid Electric Vehicles, IEEE Transactions on Power Electronics 27 (1) (2012) 122–132. doi:10.1109/TPEL.2011.2151206.

[24] M. Andre, The ARTEMIS European driving cycles for measuring car pollutant emissions, The Science of the total environment 334-335 (2004) 73–84. doi:10.1016/j.scitotenv.2004.04.070.